Alkoxycarbonyl elimination of 3-*O*-substituted glucose and fructose by heat treatment under neutral pH

Kazuhiro Chiku, Riku Tsukasaki, Yu Teshima, Mitsuru Yoshida, Hiroki Aramasa, Takanori Nihira, Hiroyuki Nakai, Hiroshi Ono, Motomitsu Kitaoka

PII: S0008-6215(20)30221-4

DOI: https://doi.org/10.1016/j.carres.2020.108129

Reference: CAR 108129

To appear in: *Carbohydrate Research*

Received Date: 9 April 2020

Revised Date: 6 August 2020

Accepted Date: 7 August 2020

Please cite this article as: K. Chiku, R. Tsukasaki, Y. Teshima, M. Yoshida, H. Aramasa, T. Nihira, H. Nakai, H. Ono, M. Kitaoka, Alkoxycarbonyl elimination of 3-*O*-substituted glucose and fructose by heat treatment under neutral pH, *Carbohydrate Research* (2020), doi: https://doi.org/10.1016/j.carres.2020.108129.

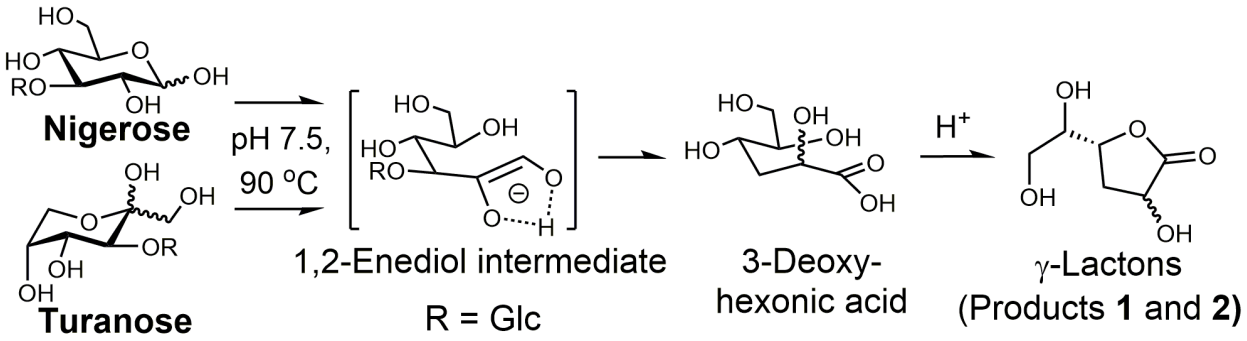

Article Type: Original Research Article

Alkoxycarbonyl elimination of 3-*O*-substituted glucose and fructose by heat treatment under neutral pH

Kazuhiro Chiku[a,*], Riku Tsukasaki[a], Yu Teshima[a], Mitsuru Yoshida[a], Hiroki Aramasa[b], Takanori Nihira[c], Hiroyuki Nakai[b,c], Hiroshi Ono[d], and Motomitsu Kitaoka[b,c,e]

[a]*Faculty of Applied Life Science, Nippon Veterinary and Life Science University, 1-7-1 Kyonancho, Musashino-shi, Tokyo 180-8602, Japan;* [b]*Graduate School of Science and Technology, and* [c]*Faculty of Agriculture, Niigata University, Niigata 950-2181, Japan*; [d]*Advanced Analysis Center, and* [e]*Food Research Institute, National Agriculture and Food Research Organization, 2-1-12 Kannondai, Tsukuba, Ibaraki 305-8642, Japan.*

[*]Corresponding author: Kazuhiro Chiku (Tel. +81-422-31-4151, Fax +81-422-33-2094, E-mail chiku@nvlu.ac.jp, and ORCID ID 0000-0001-6857-8894)

Abstract

3-*O*-Substituted reducing aldoses are commonly unstable under heat treatment at neutral and alkaline pH. In this study, to evaluate the decomposition products, nigerose (3-*O*-α-D-glucopyranosyl-D-glucose) and 3-*O*-methyl glucose were heated at 90 °C in 100 mM sodium phosphate buffer (pH 7.5). Decomposition via β-elimination was observed that formed a mixture of 3-deoxy-*arabino*-hexonic acid and 3-deoxy-*ribo*-hexonic acid; upon further acid treatment, it was converted to their γ-lactones. Similarly, turanose (3-*O*-α-D-glucopyranosyl-D-fructose), a ketose isomer of nigerose, decomposed more rapidly than nigerose under the same conditions, forming the same products. These findings indicate that 3-*O*-substituted reducing glucose and fructose decompose via the same 1,2-enediol intermediate. The alkoxycarbonyl elimination of 3-*O*-substituted reducing glucose and fructose occurs readily if an *O*-glycosidic bond is located on the carbon adjacent to the 1,2-enediol intermediate. Following these experiments, we proposed a kinetic model for the decomposition of nigerose and turanose by heat treatment under neutral pH conditions. The proposed model showed a good fit with the experimental data collected in this study. The rate constant of the decomposition for nigerose was $(1.2 \pm 0.1) \times 10^{-4}$ s^{-1}, whereas that for turanose [$(2.6 \pm 0.2) \times 10^{-4}$ s^{-1}] was about 2.2 times higher.

Keywords

Alkoxycarbonyl elimination; Enediol intermediate; Nigerose; Turanose;

3-Deoxy-hexonic acid

1. Introduction

Oligosaccharides are functional food ingredients that improve the quality of many foods [1–3]. Some confer physicochemical characteristics such as textural and organoleptic properties and others afford beneficial properties for human health such as improving digestibility, promoting the growth of beneficial bacteria in the colon (probiotic effects) [2], and boosting the human immune system [4,5]. Given the popularity of foods with proven health effects, the demand for food products containing functional oligosaccharides will inevitably increase, and some oligosaccharides are added to food ingredients before heat processing [1,6]. Although heating can decrease the microbiological risk and improve the shelf life and digestibility of foods, this process causes the decomposition of oligosaccharides. To control this reaction, understanding the non-enzymatic decomposition of oligosaccharides in foods is an important issue in food processing. Therefore, we investigated the stability of various oligosaccharides under neutral pH conditions by heat treatment below 100 °C, kinetic parameters of the transformation reactions, and temperature and pH dependences of the reaction rate [7,8].

In previous study, we evaluated the heat stability of 3-*O*-β-D-galactopyranosyl-D-2-acetamido-2-deoxy-D-glucose (lacto-*N*-biose I) [7]. Lacto-*N*-biose I is a growth-promoting factor of infant-specific bifidobacteria in human milk [9] and has the potential to be used as a food or food additive. However, lacto-*N*-biose I rapidly decomposed with water elimination during heating under neutral pH conditions in which glycosyl linkages are generally believed to be stable [7]. This

undesirable reaction is known as β-elimination, and in higher degrees of oligosaccharide and polysaccharide, it is sometimes referred to as “peeling reaction” because it proceeds until the alkali-stable glycosidic linkage appears at the reducing end. The thermal instability of lacto-*N*-biose I under neutral pH extended to the instability of oligosaccharides with a 3-*O*-substituted reducing aldose, including nigerose (3-*O*-α-D-glucopyranosyl-D-glucose) [7].

Nigerose is the constitutional unit of α-1,3-glucans produced in the cell wall of filamentous fungi [10,11] and fission yeast [12], which are sometimes used in the fermentation process. As a result of these fermentation processes, nigerose is also present in fermentation products in Japanese rice wine [13], and beer [14]. Our previous study showed that nigerose and α-1,3-oligosaccharides (nigerooligosaccharides) can be prepared using nigerose phosphorylase and α-1,3-oligoglucan phosphorylase [15–17].

The ketose isomer of nigerose is turanose (3-*O*-α-D-glucopyranosyl-D-fructose), which occurs naturally in honey, along with nigerose [18,19]. Turanose has about half the sweetness of sucrose [20], is non-cariogenic [21,22], has beneficial effects in controlling adipogenesis [23], and has anti-inflammatory effects [24]. As an inhibitor of acid α-glucosidase, turanose is also used for the medical diagnosis of Pompe’s disease [25]. Turanose can be synthesized from a mixture of cyclomaltohexaose (α-cyclodextrin) and fructose via two enzymatic steps with cyclomaltodextrin glucanotransferase and glucoamylase [20] or can be synthesized from high concentration sucrose by amylosucrase [26].

Turanose does not have a hydrogen atom at the β-position (C-2) and therefore

cannot undergo β-elimination like nigerose. If turanose has heat stability, it may have the potential as a new functional sweetener that can be used in heat-processed foods. In addition, the aldose–ketose reaction from turanose could be an efficient source of nigerose synthesis. However, turanose is more unstable to heat than nigerose and rapid decomposition was observed.

In this study, in addition to the decomposition products of nigerose, the structure of which are not yet known, the decomposition products of turanose and their reaction mechanisms were also investigated. We further determined the kinetic parameters and investigated the temperature and pH dependence for the thermal decompositions of nigerose and turanose.

2. RESULTS

2.1. Heat treatment of nigerose, nigerotriose, and 3-O-methyl glucose at neutral pH

Nigerose, nigerotriose, or 3-*O*-methyl glucose (initial concentration, 50 mM) as the single substrate was heated in 100 mM sodium phosphate buffer (pH 7.5) at 90 °C. TLC analysis of the reaction solutions showed that nigerose and nigerotriose decomposed concomitantly with the release of glucose and nigerose, respectively, at the beginning of the reaction (Fig. 1A and B) but heat treatment of 3-*O*-methyl glucose did not release glucose (Fig. 1C). These data show that these 3-*O*-substituted reducing glucoses undergo decomposition via β-elimination of the alkoxycarbonyl moieties.

TLC spots with similar Rf values were observed in reaction mixtures from nigerose, nigerotriose, and 3-*O*-methyl glucose (Fig. 1A–C). Fractions corresponding to the spots

in the reaction solution of nigerose and 3-*O*-methyl glucose were separated by silica gel column chromatography and desalted using Amberlite MB-4 (Organo Co., Tokyo, Japan), a mixture of free strongly acidic and basic resins. Liquid chromatography-electrospray ionization mass spectrometry (LC-ESIMS) of the fractions showed a peak at *m/z* 161 corresponding to the mass of a deprotonated molecular ion $[M–H]^-$ of hexose mono-dehydrate. The ^1H and ^{13}C NMR spectra of the three fractions (Fig. S1) suggest that the fractions contain two major compounds (products **1** and **2**) and that these two compounds are present in all three fractions, as the spectra are identical. The fraction from 3-*O*-methyl glucose was analyzed by DQF-COSY, TOCSY, HSQC, and HMBC methods (Fig. S2). The assignments of the ^1H and ^{13}C NMR chemical shifts of products **1** and **2** are summarized in Table 1. We identified their structures as γ-lactones of 3-deoxy-*arabino*-hexonic acid (product **1**) and 3-deoxy-*ribo*-hexonic acid (product **2**). Their ^{13}C NMR spectra show characteristic carbonyl carbons at δ 182.2 and δ 182.7, and the signals derived from C-4 were observed at δ 80.1 and δ 81.9. The presence of carbonyl groups and the downfield shifts of C-4 suggest the formation of γ-lactone between C-1 and C-4 in products **1** and **2**, considered together with their molecular weights; however, a long-range C-H correlation of C-1─H-4 was not observed in their HMBC spectra. Observing cross peaks on HMBC spectra can be difficult if the dihedral angle between the carbon and proton is close to 90°, as in the case of γ-lactone. The mixture of products **1** and **2** was hydrolyzed to the corresponding 3-deoxy-hexonic acids by heat treatment with 100 mM potassium carbonate in deuterium oxide (D_2O), as previously described [27]. The ^1H

NMR spectra of the hydrolysate contained a set of signals consistent with those of the reference standard 3-deoxy-*arabino*-hexonic acid (Toronto Research Chemicals Inc., Toronto, Canada) (Fig. S3). This result confirmed that product 1 is γ-lactone of 3-deoxy-*arabino*-hexonic acid. As the authentic 3-deoxy-*ribo*-hexonic acid was not available, whether product **2** gives this acid by hydrolysis has not been proved in this study.

All of the silica gel column chromatography fractions from the heat-treated 3-*O*-substited reducing glucoses contained the γ-lactone of 3-deoxy-*arabino*-hexonic acid and 3-deoxy-*ribo*-hexonic acid in a ratio of 2:1. In the LC-ESIMS spectra, a peak at *m/z* 179 was also observed and corresponds to the mass value of hexonic acids. No peaks corresponding to free 3-deoxy-hexonic acid were detected in ^{1}H or ^{13}C NMR. This observation suggests that γ-lactone hydrolysis occurs through electrospray ionization. In addition, 3-*O*-methyl fructose was found in the reaction product from 3-*O*-methyl glucose (Fig. 1C), resulting from keto-aldose transformation of glucose into fructose [28].

2.2. Heat treatment of turanose at neutral pH

Turanose (50 mM) was heated in 100 mM sodium phosphate buffer (pH 7.5) at 90 °C. TLC analysis revealed a new spot not corresponding to glucose or turanose. The Rf value of the new spot was similar to those of the decomposition products from the 3-*O*-substituted glucoses described above (Fig. 1D). The ^{1}H and ^{13}C NMR spectra of the fraction corresponding to the spot were identical to those containing a mixture of products **1** and **2** (Fig. S1). The ratio of products **1** and **2** was 2:1, identical to that

observed for the decomposition products from the 3-*O*-substitued glucoses described above. These data indicate that the nigerose and turanose decomposed through the same pathway. Notably, turanose has a glycosidic bond at the C-3 position that precludes the presence of a hydrogen at the β position from the leaving group. Thus, this reaction is categorized as γ-hydrogen elimination, not β-hydrogen elimination.

2.3. Time-dependent changes in NMR spectra of the reaction mixtures

To determine the mechanism that generated the γ-lactone structure in products **1** and **2**, time-dependent changes in ^{1}H NMR spectra of the reaction mixtures during heat treatment were analyzed. The signals derived from H-3 and H-3' of 3-deoxy-hexonic acids of products **1** and **2** were observed in the range of δ 1.7–2.1 in a ratio of 9:2 (Fig. 2A–C). No signals corresponding to the γ-lactone forms of products **1** and **2** were detected. To determine whether γ-lactones form due to the presence of acid, reaction mixtures after heat treatment for 360 min were treated by hydrogen form of Amberlite IR120B. Signals derived from 3-deoxy-hexonic acid forms were completely absent, and those derived from γ-lactone forms were present (Fig. 2D). This result indicates that the γ-lactones formed from 3-deoxy-hexonic acids during treatment with Amberlite MB-4. In addition, products **1** and **2** in 100 mM sodium phosphate were slowly hydrolyzed from γ-lactone forms to 3-deoxy-hexonic acid forms under mild conditions at room temperature (Fig. S4). In cases of heat treatment of nigerose in D_2O, the ^{1}H NMR signals derived from H-3 and H-3' of the 3-deoxy-hexonic acids had completely disappeared, and the signals derived from H-2 were observed as a singlet (Fig. 3), indicating that protons at the C-3 but not C-2 position of 3-deoxy-hexonic acids were

substituted by deuterium (Fig. 4). This result suggests that the protons on C-3 migrated from C-1 of the aldehyde intermediate during nigerose decomposition.

2.4. Reaction mechanism and kinetics of heat decomposition of nigerose and turanose

HPLC analysis of the decomposition reaction solutions showed that the amounts of nigerose and turanose gradually decreased, concomitant with the release of an equimolar, not double molar, amount of glucose (Fig. 5). Unfortunately, 3-deoxy-*arabino*-hexonic and 3-deoxy-*ribo*-hexonic acids were not detectable on HPLC equipped with an amino-based column. After a 720-min incubation, pH of the reaction solutions of nigerose and turanose decreased to pH 6.4 and 6.1, respectively, from pH 7.5 (Fig. 5). This observation is attributed to the generation of 3-deoxy-hexonic acids.

Herein, we propose a mechanism for the aldose–ketose tautomerization and the alkoxycarbonyl elimination of nigerose (substrate **1**) and turanose (substrate **2**) through a 1,2-enediol intermediate under neutral pH conditions, as illustrated in Fig. 6. Some aldose–ketose tautomerization between nigerose and turanose can occur; however, alkoxycarbonyl elimination preferentially occurs on the carbon adjacent to the 1,2-enediol intermediate. Keto-enol tautomerization and benzylic acid rearrangement after the elimination can occur, resulting in a mixture of 3-deoxy-*arabino*-hexonic and 3-deoxy-*ribo*-hexonic acids and subsequent formation of their γ-lactones (Products **1** and **2**) in the presence of acid. The simplified scheme is shown by the dotted arrows in Fig. 6. The observed decomposition reactions did not proceed with simple first-order reactions, evidenced by the non-linear relationship between time and log [S] (Fig. S5).

The first-order rate constant is a function of pH and decreases with a decrease in pH. We therefore constructed a new equation based on the assumption that the first-order rate constant of the elimination decreases in the same way as the first-order reaction, resulting in the following formula:

$$d[S]/dt = -k \times \exp(-a \times t) \times [S]$$

where k is the first-order rate constant of decomposition at the initial pH and a is the first-order rate constant of the decrease in the elimination rate constant. The following equation is available by integrating the formula with the boundary conditions where $t = 0$, $[S] = [S]_0$:

$$[S] = [S]_0 \times \exp\{-(k/a) \times [1 - \exp(-a \times t)]\} \quad (1)$$

This equation well fitted the experimental data (Fig. S6). The rate constant k for the decomposition for nigerose in 100 mM sodium phosphate buffer (pH 7.5) at 90°C was $(1.2 \pm 0.1) \times 10^{-4}$ s^{-1} and that for turanose was about 2.2 times higher [$(2.6 \pm 0.2) \times 10^{-4}$ s^{-1}].

2.5. Temperature and pH dependence of decomposition rate for nigerose and turanose

The rate constants for the decomposition reactions increased exponentially with temperature (Fig. 7). At a temperatures of 75 °C, no decomposition of either nigerose or turanose was observed (about 90% remaining) within 60 min. The activation energy (E_a) calculated for the decomposition of nigerose was 159 ± 17 kJ mol^{-1}, a value nearly identical to that of turanose (160 ± 27 kJ mol^{-1}).

The pH dependence of the decomposition reaction for nigerose and turanose was

studied at 90 °C in 100 mM sodium phosphate buffers (pH range, 6.0–8.5). Previously, we reported that the decomposition and isomerization reaction rates are dependent on the concentration of the hydroxide ion, regardless of the type of buffer, except for borate buffer [7,8]. We observed here that the rate constants for the decomposition reaction increased exponentially with increasing pH. High correlation coefficients (0.99) were observed between $\log_{10}k$ and pH for nigerose and turanose (Fig. 8). Nigerose and turanose were stable at pH 6.5 and 90 °C for 1 h (remaining amount ≥ 90%).

3. DISCUSSION

This study investigates the behavior of nigerose and turanose during heating at temperatures below 100 °C under neutral pH, conditions under which glycosyl linkages were assumed to be stable. We observed that nigerose and turanose rapidly decomposed at pH 7.5 and 90 °C, forming 3-deoxy-*arabino*-hexonic and 3-deoxy-*ribo*-hexonic acid. The pH dependence of the reaction rates indicate that the alkoxycarbonyl elimination reaction, which is usually seen under strong alkaline conditions, also occurs at neutral pH. Under alkaline conditions, degradation of 3-*O*-substituted glucose occurs via the Nef–Isbell mechanism [29]. In the case of 3-*O*-substituted glucose, β-elimination is followed by keto-enol tautomerization and then benzylic acid rearrangement, resulting in a mixture of 3-deoxy-*arabino*-hexonic and 3-deoxy-*ribo*-hexonic acids [29]. During heat treatment of nigerose in D_2O, protons at the C-3 position of 3-deoxy-*arabino*-hexonic and 3-deoxy-*ribo*-hexonic acids were substituted with deuterium via keto-enol tautomerism; the proton at the C-2 position was not substituted

because it is not involved in the tautomerization. This result is consistent with a reaction mechanism described in a previous report [30]. In the present study, we first identified two γ-lactones as products of decomposition of 3-*O*-substited reducing glucose and fructose. These γ-lactones were later revealed to form during acid treatment of the 3-deoxy-hexonic acids generated by the decomposition reaction. In addition, 3-deoxy-2,3-unsaturated compounds and bicyclic 3,6-anhydrofuranoses, which are observed as decomposition products of 3-*O*-substituted 2-acetamido-2-deoxy-D-hexose [7] and 2-*O*-substituted glucose such as kojibiose [8], are not major products from nigerose or turanose. These products cannot form because the reaction rates of keto-enol tautomerism and benzylic acid rearrangement are faster than those that form bicyclic compounds.

Alkoxycarbonyl elimination is known to occur readily in molecules containing an aldehyde carbonyl group located one carbon apart from an *O*-glycosidic bond as the leaving group. In this study, we found that alkoxycarbonyl elimination also occurs if a ketone carbonyl group is neighbors the *O*-glycosidic bond. In the case of 2-*O*-substituted glucose, as in kojibiose and sophorose in which an aldehyde carbonyl group neighbors the *O*-glycosidic bond, elimination of the *O*-glycosidic bond did not occur [8]. This difference depends on the capacity to form a 1,2-enediol structure as a common intermediate between 3-*O*-substituted aldose and ketose. In the case of kojibiose and sophorose, the 1,2-enediol intermediate cannot be generated because the 2-*O*-hydroxy group is blocked, and the glucose residue is directly converted into a mannose residue [8].

We conclude that 3-*O*-substituted reducing aldoses and ketose generally decompose via elimination of an *O*-substituent under neutral and alkaline conditions during heating. Elimination of a 3-*O*-substituent can occur easily if the *O*-glycosidic bond is located on the carbon adjacent to a 1,2-enediol structure as the common intermediate. These findings regarding the behavior of nigerose and turanose under heating will be useful in the development of production and application methods for oligosaccharides with 1,3-glycosidic bonds.

4. MATERIALS AND METHODS

4.1 Materials

Nigerose and nigerotriose were prepared using nigerose phosphorylase [15] and α-1,3-oligoglucan phosphorylase [17], respectively, as we previously reported. Nigerose was purchased from Carbosynth Limited (Berkshire, UK). Turanose was purchased from Tokyo Chemical Industry (Tokyo, Japan). 3-*O*-Methyl glucose was purchased from FUJIFILM Wako Pure Chemical Corporation (Osaka, Japan). 3-Deoxy-*arabino*-hexonic acid (calcium salt) was purchased from Toronto Research Chemicals Inc. (Toronto, Canada). Other chemicals used were of reagent grade.

4.2. Heat treatment of sugars

The sugars were dissolved to approximately 50 mM in 100 mM sodium phosphate buffer (pH 7.5) as standard conditions of preparation. The solutions (25 μL) were placed in a 200-μL thermal tube and heated at 90 °C for 0, 30, 60, 120, 180, 360, or 720 min in an Astec PCR Thermal Cycler PC-708 (Astec Cell Science Research Laboratory,

Fukuoka, Japan). The reaction mixture solutions were analyzed by HPLC to identify the starting substrate and its products.

4.3. TLC analysis

The reaction mixture (1 μL) was spotted on a TLC plate (TLC Silica gel 60 F_{254}; 5 × 7.5 cm, Merck KGaA, Darmstadt, Germany), and the plate was developed twice with *n*-propanol/water/28% ammonium hydroxide (14:3:3, by volume) as the solvent phase. After development, the plate was dipped in a solution of sulfuric acid/*p*-anisaldehyde/acetic acid/ethanol (18:13:5:478, by volume) and heated in an oven to detect the compounds.

4.4. HPLC analysis

The sugar compositions were determined using an HPLC system (Shimadzu, Kyoto, Japan) equipped with a RefractoMax 521 refractive index detector (ERC Inc., Saitama, Japan) using a Shodex HILICpak VG-50 column (4.6 mm i.d. × 250 mm; Showa Denko, Tokyo, Japan) at 40 °C under a constant flow (0.8 mL/min) of 75% acetonitrile in water as the mobile phase.

4.5. Isolation of reaction products from nigerose

Nigerose (34.2 mg, 100 μmol) was dissolved in 2 mL of 100 mM sodium phosphate buffer (pH 7.5), and the solution was incubated at 90 °C for 12 h. The reaction mixture was desalted using Amberlite MB-4 (approximately 500 mg), passed through a Sep-Pak plus C18 cartridge (360 mg of sorbent; Waters, Milford, MA), lyophilized, and resolved with 90% acetonitrile in water. The products in the reaction mixture were isolated by using an HPLC system equipped with a Wakosil 5SIL column (10 mm i.d. × 250 mm;

FUJIFILM Wako Pure Chemical Corporation) at 40 °C under a constant flow (2.0 mL/min) of 85% acetonitrile in water as the mobile phase. The three major peaks eluted at 16.3 min (fraction 1), 19.6 min (glucose), and 22.8 min (nigerose). The eluate of the peak corresponding to fraction 1 was collected and lyophilized to obtain 1.6 mg of solid.

4.6. Isolation of reaction products from 3-O-methyl glucose

3-*O*-Methyl glucose (38.8 mg, 200 μmol) was dissolved in 4 mL of 100 mM sodium phosphate buffer (pH 7.5), and the solution was incubated at 90 °C for 12 h. Reaction products were isolated following the same process as for nigerose. The HPLC chromatogram showed three major peaks, eluting at 14.9 min (fraction 2), 15.7 min (3-*O*-methyl glucose), and 16.3 min (3-*O*-methyl fructose). These fractions were collected and lyophilized. The eluate of the peak corresponding to fraction 2 was collected and lyophilized to obtain 2.6 mg of solid.

4.7. Isolation of reaction products from turanose

Turanose (34.2 mg, 100 μmol) was dissolved in 2 mL of 100 mM sodium phosphate buffer (pH 7.5), and the solution was incubated at 90 °C for 12 h. The reaction products were isolated following the same process as for nigerose. The HPLC chromatogram revealed three major peaks, eluting at 16.3 min (fraction 3), 19.6 min (glucose), and 22.6 min (turanose). The eluate of the peak corresponding to fraction 3 was collected and lyophilized to obtain 1.0 mg of solid.

4.8. NMR and ESI-MS measurements

^{1}H and ^{13}C NMR spectra were obtained in D_2O on an Avance 800 spectrometer (Bruker BioSpin GmbH, Rheinstetten, Germany). Chemical shifts for ^{1}H and ^{13}C NMR signals are given in D_2O at 298.15 K, with 3-(trimethylsilyl)propionic-2,2,3,3-d_4 acid as an internal standard (δ_H 0.00 and δ_C 0.00). The following abbreviations are used for the characterization of NMR signals: s, singlet; d, doublet; t, triplet; and m, multiplet. ESIMS spectra were recorded on a Velos Pro Dual-Pressure Linear Ion Trap Mass Spectrometer (Thermo Fisher Scientific Inc., Waltham, MA) and an API 2000 LC/MS/MS (AB Sciex, Framingham, MA, USA).

4.9. Spectroscopic data of fraction 1 from nigerose (Products 1 and 2)

ESI(+)-MS: *m/z* 185.00 $[M+Na]^+$ (calculated for $C_6H_{10}O_5Na^+$, 185.04), *m/z* 203.00 $[M+H_2O+Na]^+$ (calculated for $C_6H_{12}O_6Na^+$, 203.05), *m/z* 347.03 $[2M+Na]^+$ (calculated for $C_{12}H_{20}O_{10}Na^+$, 347.09). ESI(−)-MS: *m/z* 161.05 $[M-H]^-$ (calculated for $C_{12}H_{15}O_{10}^-$, 161.05), *m/z* 179.03 $[M+H_2O-H]^-$ (calculated for $C_6H_{15}O_6^-$, 179.06). ^{1}H and ^{13}C NMR spectra are shown in Fig. S1.

4.10. Spectroscopic data of fraction 2 from 3-O-methyl glucose (products 1 and 2)

ESI(+)-MS: *m/z* 185.01 $[M+Na]^+$ (calculated for $C_6H_{10}O_5Na^+$, 185.04), *m/z* 203.08 $[M+H_2O+Na]^+$ (calculated for $C_6H_{12}O_6Na^+$, 203.05), *m/z* 347.07 $[2M+Na]^+$ (calculated for $C_{12}H_{20}O_{10}Na^+$, 347.09). ESI(−)-MS: *m/z* 161.07 $[M-H]^-$ (calculated for $C_{12}H_{15}O_{10}^-$, 161.05), *m/z* 179.06 $[M+H_2O-H]^-$ (calculated for $C_6H_{15}O_6^-$, 179.06). ^{1}H and ^{13}C NMR spectra are shown in Figs. S1 and S2. The NMR assignments are shown in Table 1.

4.11. Spectroscopic data of the reaction product from 3-O-methyl glucose (3-O-methyl fructose)

ESI(+)-MS (API 2000): *m/z* 195.0 $[M+H]^+$ (calculated for $C_7H_{14}O_6H^+$, 195.18). ESI(−)-MS (API 2000): *m/z* 193.3 $[M-H]^-$ (calculated for $C_7H_{13}O_6^-$, 193.18). ^1H and ^{13}C NMR spectra are shown in Fig. S7.

4.12. Spectroscopic data of fraction 3 from turanose (products 1 and 2)

ESI(+)-MS: *m/z* 163.06 $[M+H]^+$ (calculated for $C_6H_{10}O_5H^+$, 163.05), *m/z* 185.00 $[M+H_2O+Na]^+$ (calculated for $C_6H_{10}O_5Na^+$, 185.04), *m/z* 203.00 $[M+Na]^+$ (calculated for $C_6H_{12}O_6Na^+$, 203.05), *m/z* 347.04 $[2M+Na]^+$ (calculated for $C_{12}H_{20}O_{10}Na^+$, 347.09). ESI(−)-MS: *m/z* 161.06 $[M-H]^-$ (calculated for $C_{12}H_{15}O_{10}^-$, 161.05), *m/z* 179.05 $[M+H_2O-H]^-$ (calculated for $C_6H_{15}O_6^-$, 179.06). ^1H and ^{13}C NMR spectra are shown in Fig. S1.

4.13. Hydrolysis of γ-lactones

Approximately 1 mg of lyophilized products derived from fraction 2 was dissolved in 100 mM potassium carbonate in D_2O (0.6 mL) and heated at 80 °C for 60 min. The ^1H NMR spectrum of the reaction mixture was recorded on the Avance 800 spectrometer.

4.14. Time-dependent changes in NMR spectra of the reaction mixtures.

Nigerose was dissolved to approximately 50 mM in 100 mM sodium phosphate buffer (pH 7.5) in water or D_2O. The solutions (200 μL) were placed in a 200-μL thermal tube and heated at 90 °C for 0, 120, or 360 min in an Astec PCR Thermal Cycler PC-708. The reaction mixture after heat treatment for 360 min was treated with the hydrogen form of Amberlite IR120B (approximately 50 mg). In the case of water, the reaction mixture were lyophilized, resolved with deuterium oxide, and analyzed by

^{1}H NMR spectroscopy. The ^{1}H NMR spectrum of the reaction mixture in deuterium oxide was recorded on the Avance 800 spectrometer.

4.15. Determination of kinetic parameters

The rate constant (k) of the decomposition was calculated by regressing data with equation (1) using Origin 2018 (LightStone Corp., Tokyo, Japan).

The apparent energy of activation (E_a) was obtained by regressing data with the Arrhenius Equation (2), where A, R, and T are frequency factors, the gas constant, and absolute temperature, respectively, again using Origin 2018:

$$\ln k = \ln A - E_a / (R \times T) \quad (2)$$

4.16. Influence of temperature and pH on decomposition of nigerose and turanose

The effect of temperature on the decomposition of nigerose and turanose was measured under the standard condition described above at temperatures of 70, 75, 80, 85, 90, and 95 °C. The effect of pH on the decomposition of nigerose and turanose was measured under the standard condition described above using 100 mM sodium phosphate buffer (pH 6.0, 6.5, 7.0, 7.5, 8.0, or 8.5). The concentration of the nigerose or turanose reduced with heat treatment was sequentially measured using the HPLC method described above.

Funding

Part of this work was supported by JSPS KAKENHI Grant Numbers JP15K18705 and JP17K15251.

Declaration of competing interests

We have no conflict of interests to declare.

Acknowledgments

The NMR and MS spectra were recorded by the staff at the Advanced Analysis Center, NARO. The authors would like to thank Enago (www.enago.jp) for the English language review.

REFERENCES

[1] Z. Zdunczyk, Physiological effect of low digestible oligosaccharides in diets for animals and humans, Polish J. Food Nutr. Sci. 13 (2004) 115–130.

[2] S.I. Mussatto, I.M. Mancilha, Non-digestible oligosaccharides: A review, Carbohydr. Polym. 68 (2007) 587–597. https://doi.org/10.1016/j.carbpol.2006.12.011.

[3] X. Qiang, C. YongLie, W. QianBing, Health benefit application of functional oligosaccharides, Carbohydr. Polym. 77 (2009) 435–441. https://doi.org/10.1016/j.carbpol.2009.03.016.

[4] A. Rijnierse, P. V. Jeurink, B.C.A.M. van Esch, J. Garssen, L.M.J. Knippels, Food-derived oligosaccharides exhibit pharmaceutical properties, Eur. J. Pharmacol. 668 (2011) S117–S123. https://doi.org/10.1016/j.ejphar.2011.07.009.

[5] A.J. Nauta, J. Garssen, Evidence-based benefits of specific mixtures of non-digestible oligosaccharides on the immune system, Carbohydr. Polym. 93 (2013) 263–265. https://doi.org/10.1016/j.carbpol.2012.02.021.

[6] D. Charalampopoulos, R.A. Rastall, Prebiotics in foods, Curr. Opin. Biotechnol. 23 (2012) 187–191. https://doi.org/10.1016/j.copbio.2011.12.028.

[7] K. Chiku, M. Nishimoto, M. Kitaoka, Thermal decomposition of β-D-galactopyranosyl-(1→3)-2-acetamido-2-deoxy-D-hexopyranoses under neutral conditions, Carbohydr. Res. 345 (2010) 1901–1908. https://doi.org/10.1016/j.carres.2010.06.003.

[8] K. Chiku, M. Wada, H. Atsuji, A. Hosonuma, M. Yoshida, H. Ono, M. Kitaoka,

Epimerization and decomposition of kojibiose and sophorose by heat treatment under neutral pH conditions, J. Appl. Glycosci. 66 (2019) 1–9. https://doi.org/10.5458/jag.jag.jag-2018_0002.

[9] M. Kiyohara, A. Tachizawa, M. Nishimoto, M. Kitaoka, H. Ashida, K. Yamamot, Prebiotic effect of lacto-*N*-biose I on bifidobacterial growth, Biosci. Biotechnol. Biochem. (2009). https://doi.org/10.1271/bbb.80697.

[10] A. Yoshimi, K. Miyazawa, K. Abe, Function and biosynthesis of cell wall α-1,3-glucan in fungi, J. Fungi. 3 (2017) 63. https://doi.org/10.3390/jof3040063.

[11] I. Johnston, The composition of the cell wall of *Aspergillus niger*, Biochem. J. 96 (1965) 651–658. https://doi.org/10.1042/bj0960651.

[12] J.H. Sietsma, J.G.H. Wessels, The occurrence of glucosaminoglycan in the wall of *Schizosaccharomyces pombe*, J. Gen. Microbiol. 136 (1990) 2261–2265. https://doi.org/10.1099/00221287-136-11-2261.

[13] Y. Nunokawa, Oligosaccharides in sake, J. Japanese Soc. Starch Sci. 28 (1981) 109–117. https://doi.org/10.5458/jag1972.28.109.

[14] K. Aso, T. Waranabe, Studies on beer. Part II. Gluco-bioses in beer., J. Agric. Chem. Soc. Japan. 35 (1961) 1078–1082. https://doi.org/10.1271/nogeikagaku1924.35.11_1078.

[15] T. Nihira, H. Nakai, K. Chiku, M. Kitaoka, Discovery of nigerose phosphorylase from *Clostridium phytofermentans*, Appl. Microbiol. Biotechnol. 93 (2012) 1513–1522. https://doi.org/10.1007/s00253-011-3515-9.

[16] T. Nihira, F. Miyajima, K. Chiku, M. Nishimoto, M. Kitaoka, K. Ohtsubo, H.

Nakai, One pot enzymatic production of nigerose from common sugar resources employing nigerose phosphorylase, J. Appl. Glycosci. 61 (2014) 75–80. https://doi.org/10.5458/jag.jag.JAG-2013_012.

[17] T. Nihira, M. Nishimoto, H. Nakai, K. Ohtsubo, M. Kitaoka, Characterization of two α-1,3-glucoside phosphorylases from *Clostridium phytofermentans*, J. Appl. Glycosci. 61 (2014) 59–66. https://doi.org/10.5458/jag.jag.JAG-2013_013.

[18] J. Da Costa Leite, L. Trugo, L.S. Costa, L.M. Quinteiro, O. Barth, V.M. Dutra, C.A. De Maria, Determination of oligosaccharides in Brazilian honeys of different botanical origin, Food Chem. 70 (2000) 93–98. https://doi.org/10.1016/S0956-7135(99)00115-2.

[19] K.W. Swallow, N.H. Low, Analysis and quantitation of the carbohydrates in honey using high-performance liquid chromatography, Jo. Agric. Food Chem. 38 (1990) 1828–1832. https://doi.org/10.1021/jf00099a009.

[20] T. Shibuya, T. Mandai, M. Kubota, S. Fukuda, M. Kurimoto, Y. Tsujisaka, Production of turanose by cyclomaltodextrin glucanotransferase from *Bacillus stearothermophilus*, J. Appl. Glycosci. 51 (2004) 223–227. https://doi.org/10.5458/jag.51.223.

[21] T. Minami, T. Fujiwara, T. Ooshima, Y. Nakajima, S. Hamada, Interaction of structural isomers of sucrose in the reaction between sucrose and glucosyltransferases from mutans streptococci, Oral Microbiol. Immunol. 5 (1990) 189–194. https://doi.org/10.1111/j.1399-302X.1990.tb00644.x.

[22] A. Pikis, S. Immel, S.A. Robrish, J. Thompson, Metabolism of sucrose and its

five isomers by *Fusobacterium mortiferum*, Microbiology. 148 (2002) 843–852. https://doi.org/10.1099/00221287-148-3-843.

[23] M.O. Park, B.H. Lee, E. Lim, J.Y. Lim, Y. Kim, C.S. Park, H.G. Lee, H.K. Kang, S.H. Yoo, Enzymatic process for high-yield turanose production and its potential property as an adipogenesis regulator, J. Agric. Food Chem. 64 (2016) 4758–4764. https://doi.org/10.1021/acs.jafc.5b05849.

[24] J.Y. Chung, Y.S. Kim, Y. Kim, S.H. Yoo, Regulation of inflammation by sucrose isomer, turanose, in Raw 264.7 Cells, J. Cancer Prev. 22 (2017) 195–201. https://doi.org/10.15430/JCP.2017.22.3.195.

[25] D.M. Broadhead, J. Butterworth, Pompe's disease: Diagnosis in kidney and leucocytes using 4-methylumbelliferyl-α-D-glucopyranoside, Clin. Genet. 13 (2008) 504–510. https://doi.org/10.1111/j.1399-0004.1978.tb01206.x.

[26] R. Wang, J.S. Bae, J.H. Kim, B.S. Kim, S.H. Yoon, C.S. Park, S.H. Yoo, Development of an efficient bioprocess for turanose production by sucrose isomerisation reaction of amylosucrase, Food Chem. 132 (2012) 773–779. https://doi.org/10.1016/j.foodchem.2011.11.035.

[27] M. Takenaka, X. Yan, H. Ono, M. Yoshida, T. Nagata, T. Nakanishi, Caffeic acid derivatives in the roots of Yacon (*Smallanthus sonchifolius*), J. Agric. Food Chem. 51 (2003) 793–796. https://doi.org/10.1021/jf020735i.

[28] S.J. Angyal, The Lobry de Bruyn-Alberda van Ekenstein transformation and related reactions, in: Glycosci. Top. Curr. Chem., 2001: pp. 1–14. https://doi.org/10.1007/3-540-44422-X_1.

[29] C.J. Knill, J.F. Kennedy, Degradation of cellulose under alkaline conditions, Carbohydr. Polym. 51 (2003) 281–300. https://doi.org/10.1016/S0144-8617(02)00183-2.

[30] W. Zhang, I. Carmichael, A.S. Serianni, Rearrangement of 3-deoxy-D-erythro-hexos-2-ulose in aqueous solution: NMR evidence of intramolecular 1,2-hydrogen transfer, J. Org. Chem. 76 (2011) 8151–8158. https://doi.org/10.1021/jo200288t.

Figure Legends

Figure 1. TLC analysis of reaction mixtures by heat treatment of nigerose (A), nigerotriose (B), 3-*O*-methyl glucose (C), and turanose (D) at 90 °C in 100 mM sodium phosphate buffer (pH 7.5).

The arrow on a top of plate indicates the position to which the developing solvent reached. Fru, fructose; Fru3Me, 3-*O*-methyl fructose; Glc, glucose; Glc3Me, 3-*O*-methyl glucose; Nig, nigerose, Nig3, nigerotriose; and Tur, turanose.

Figure 2. Time-dependent changes in ^{1}H NMR spectra (800 MHz) of the reaction mixtures containing nigerose by heating at 90 °C in 100 mM sodium phosphate buffer (pH 7.5).

The reaction mixture of 50 mM nigerose was heated at 90 °C for 0 min (A), 120 min (B), or 360 min (C), and then treated with the hydrogen form of Amberlite IR120B (D). 3DHA, 3-deoxy-hexonic acid.

Figure 3. Time-dependent changes in ^{1}H NMR spectra (800 MHz) of the reaction mixtures containing nigerose by heating at 90 °C in 100 mM sodium phosphate buffer (pH 7.5) and deuterium oxide.

The reaction mixture was treated at 90 °C for 0 min (A), 120 min (B), or 360 min (C).

Figure 4. Decomposition reaction of nigerose by heating at 90 °C in 100 mM sodium phosphate buffer (pH 7.5) and deuterium oxide.

D_2O, deuterium oxide.

Figure 5. Time-dependent changes in HPLC chromatogram of the reaction mixtures containing nigerose or turanose by heating at 90 °C in 100 mM sodium phosphate buffer (pH 7.5) and their quantitative evaluation.

Chromatograms (left column) obtained using HPLC systems equipped with a refractive index detector using a Shodex HILICpak VG-50 column at 40 °C with a mobile phase of 75% acetonitrile in water. Symbols in the quantitative evaluation (light column) show experimental data for the reduction of nigerose (closed circle), turanose (open circle), and pH value in the reaction mixture (open square), and the production of glucose (closed triangle) and fructose (open triangle).

Figure 6. Proposed mechanism of decomposition of nigerose and turanose into products 1 **and** 2**.**

Broken lines show the theoretical fitting curves calculated using Equation (1).

Figure 7. Arrhenius plot of the decomposition of nigerose and turanose.

The following relations for nigerose (closed circle) and turanose (open circle) were derived from a linear plot with correlation coefficients of 0.99 and 0.97, respectively. (A), $y = -19.6x + 43.5$ ($x = [1000/T]$; $y = [\ln k]$); (B), $y = -19.2x + 44.5$ ($x = [1000/T]$; $y = [\ln k]$).

Figure 8. Relationship between rate constants and pH during decomposition reactions of nigerose and turanose under heat treatment.

The following relationships for the decomposition of nigerose (A, closed circle) and turanose (B, open circle) were derived from a linear plot with correlation coefficients of 0.97. (A), $y = 0.84x - 10.3$ (x = [pH value]; $y = \log_{10}[k]$); (B), $y = 0.51x - 7.4$ (x = [pH value]; $y = \log_{10}[k]$). Reactions were conducted in 100 mM sodium phosphate buffer (pH 6.0, 6.5, 7.0, 7.5, 8.0, or 8.5). The actual pH (pH 5.7, 6.3, 6.9, 7.5, 8.1, or 8.6) in 100 mM sodium phosphate buffer was adjusted to pH 6.0, 6.5, 7.0, 7.5, 8.0, or 8.5, respectively, when heated at 90 °C.

Table 1. Chemical shifts of products **1** and **2** in ^{1}H and ^{13}C NMR spectrum of fraction 2 obtained from 3-*O*-methyl glucose under neutral pH.

Position	Product **1** (67 %)				Product **2** (33 %)			
	^{13}C δ (ppm)	^{1}H δ (ppm)	Multi.	J (Hz)	^{13}C δ (ppm)	^{1}H δ (ppm)	Multi.	J (Hz)
1	182.2	—	—	—	182.7	—	—	—
2	70.9	4.75	dd	8.7, 11.2	69.9	4.70	dd	9.0, 8.7
3	34.2	2.68	ddd	5.6, 8.7, 12.4	33.4	2.64	ddd	2.8, 9.0, 13.6
3'		2.13	ddd	10.5, 11.2, 12.4		2.26	ddd	8.7, 8.8, 13.6
4	80.1	4.60	ddd	4.5, 5.6, 10.5	81.9	4.77[a]		2.8, 4.4, 8.8
5	74.2	4.01	ddd	4.2, 4.5, 6.5	74.8	3.94	ddd	4.4, 4.6, 6.3
6	64.5	3.69	dd	4.2, 12.0	64.8	3.66	dd	4.6, 12.0
6’		3.60	dd	6.5, 12.0		3.61	dd	6.3, 12.0

a; These signals were assigned by HSQC spectrum. Multi., Multiplicity.

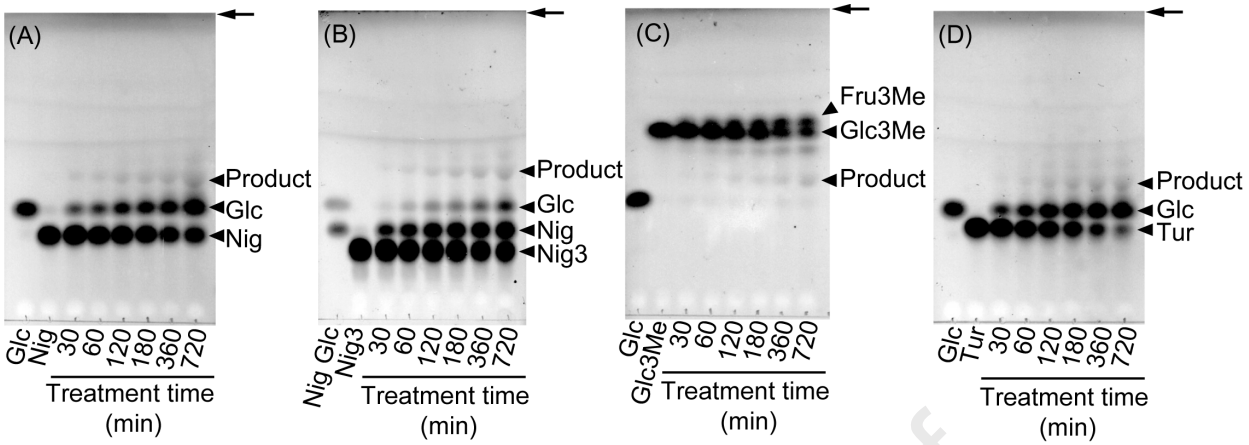

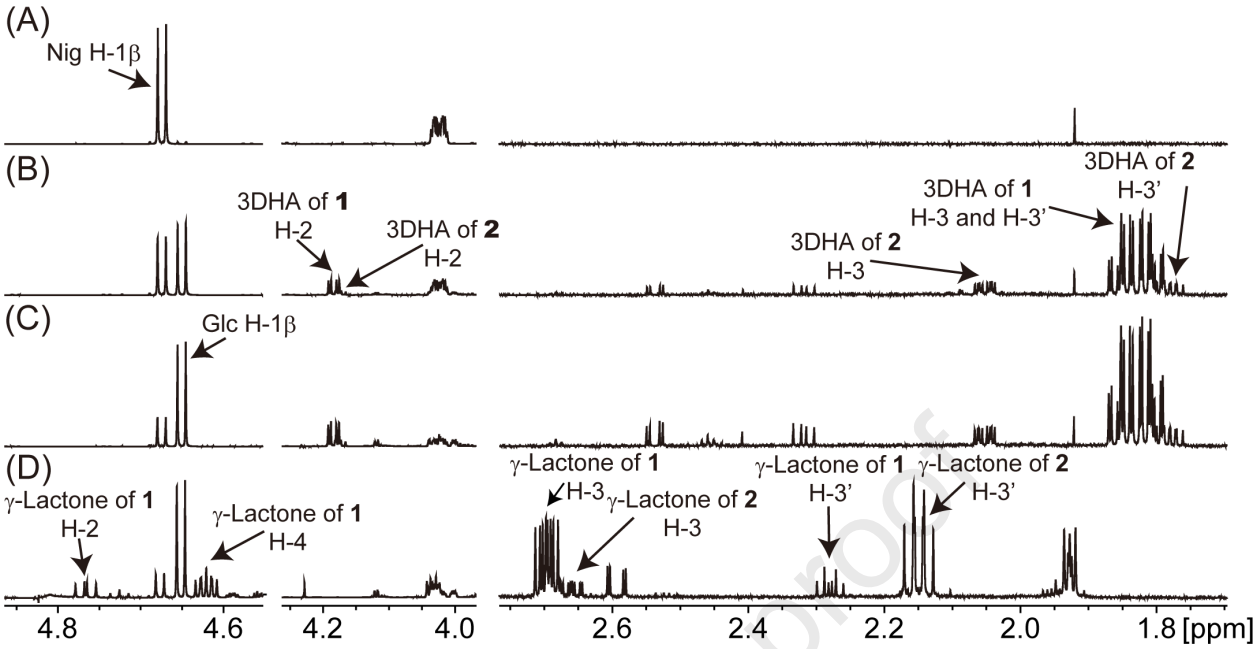

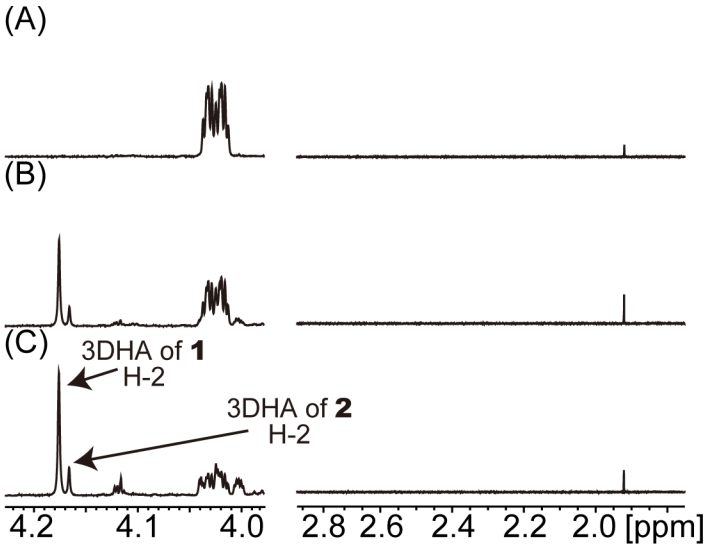

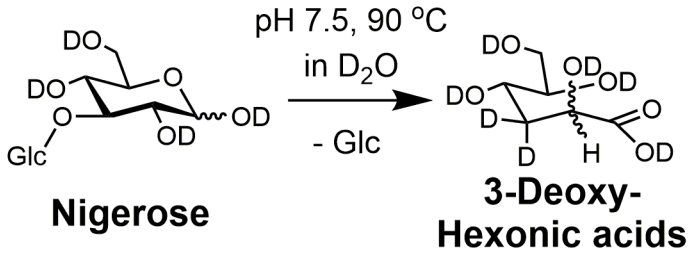

Nigerose → **3-Deoxy-Hexonic acids**

(A) Nigerose

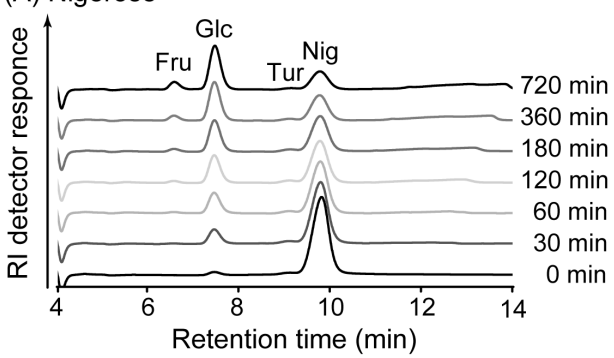

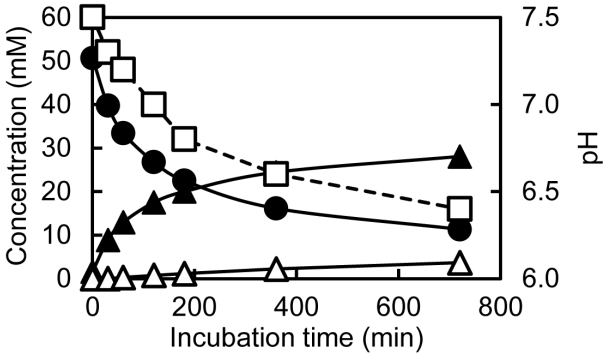

(B) Turanose

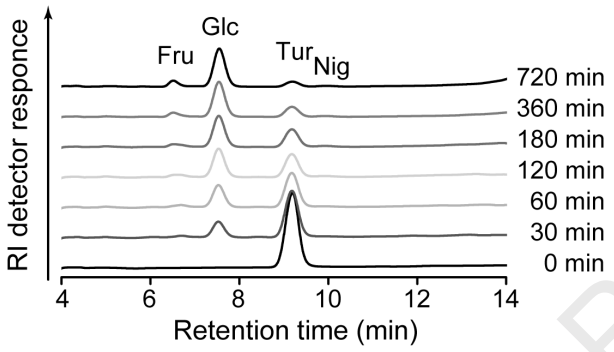

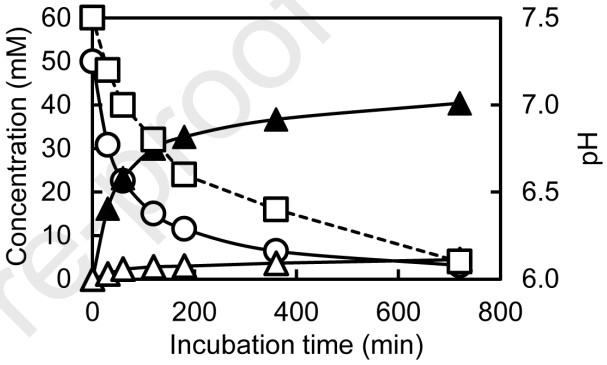

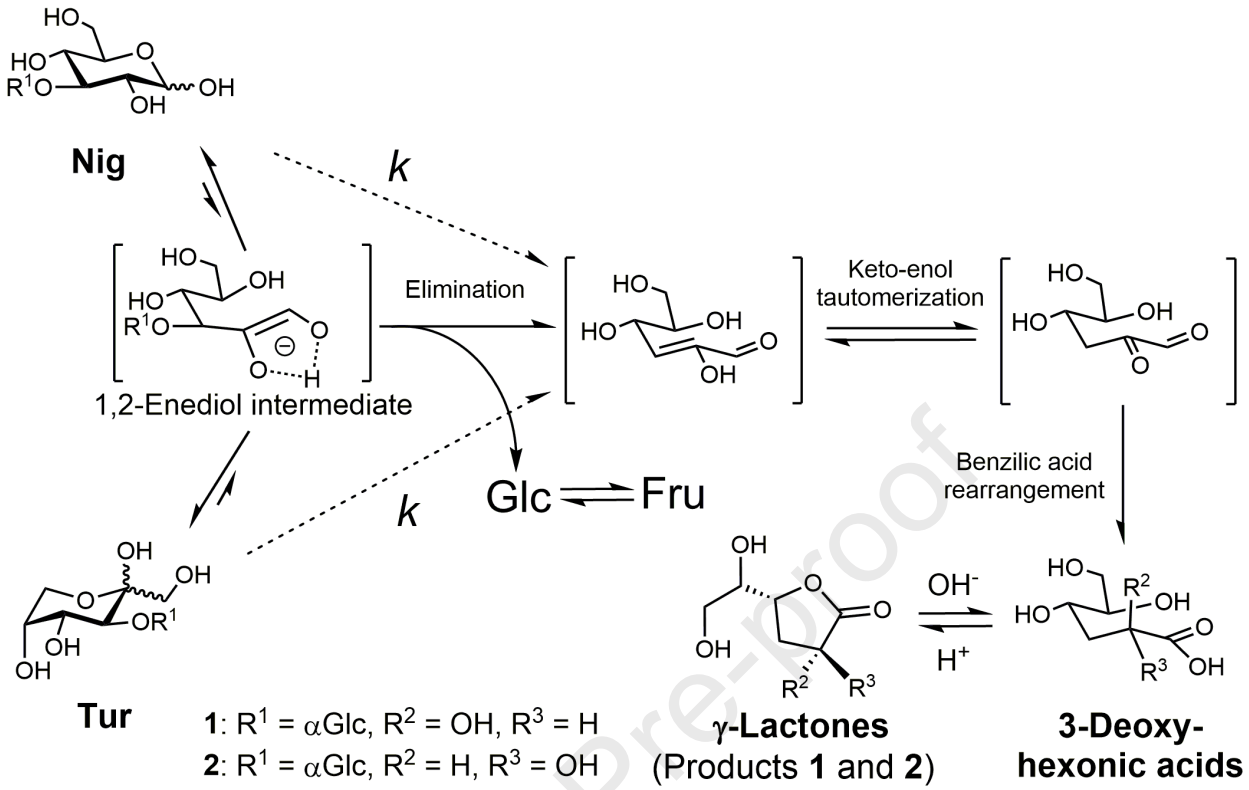

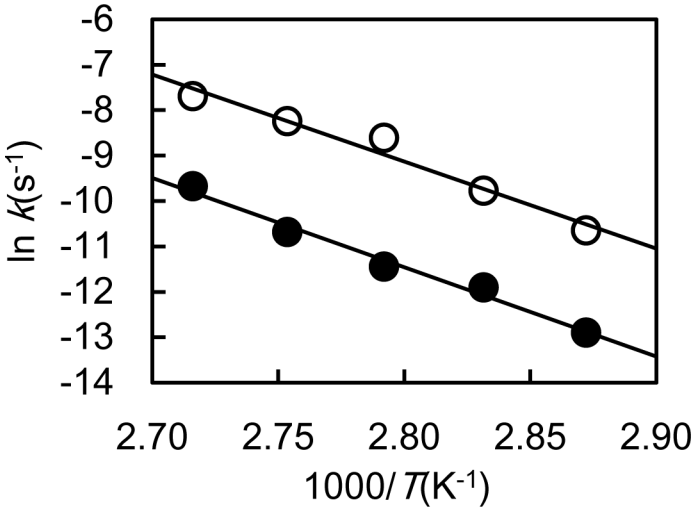

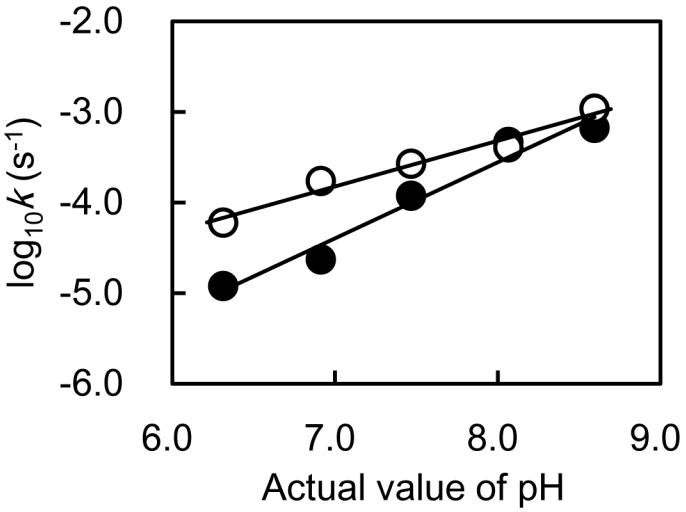

Highlights

- Nigerose and turanose are unstable against heat treatment under neutral pH.
- The decomposition by heating results in formation of 3-deoxy-hexonic acids.
- *γ*-Lactones are generated by acid treatment of 3-deoxy-hexonic acids.
- The elimination occurs on the carbon adjacent to the 1,2-enediol intermediate.

Declaration of interests

☒ The authors declare that they have no known competing financial interests or personal relationships that could have appeared to influence the work reported in this paper.

☐The authors declare the following financial interests/personal relationships which may be considered as potential competing interests: